

Long-term erosion-rate calculation from the Waipiata Volcanic Field (New Zealand) based on erosion remnants of scoria cones, tuff rings and maars

*Calcul de la vitesse d'érosion à long terme
dans la zone volcanique de Waipiata (Nouvelle-Zélande)
fondé sur les formes résiduelles de cônes de scories,
d'anneaux de tuf et de maars*

Károly Németh*

Abstract

Erosion of scoria cones, tuff rings and maars follows a general evolution. Identification of distribution patterns of preserved pyroclastic lithofacies of scoria cones, tuff rings and maars allows an estimation of "depth" of erosion since volcanism ceased. Study of the accidental lithic clast population in pyroclastic rocks of erosion remnants of basaltic maar/tuff ring volcanoes of the Miocene Waipiata Volcanic Field (WVF), in New Zealand is demonstrated to be a good tool to re-establish the "missing" stratigraphy and estimate the erosion since volcanism. An example from a subsequently tilted erosion remnant of the Swinburn multivent volcanic complex (WVF) demonstrates the importance of tilting as an effect on erosion rate calculations. The three vents of the WVF investigated from New Zealand suggest a range of erosion rates from 3.75 to 46 m/My depending on 1) the position of the remnant in comparison to uplifted fault/fold blocks; and, 2) considering or neglecting the effect of subsequent tilting on erosion rate calculations.

Key words: maar, tuff ring, scoria cone, erosion, Dunedin Volcanic Group, Waipiata Volcanic Field, New Zealand.

Résumé

L'érosion des cônes de scories, des anneaux de tuf et des maars suit une évolution générale. L'identification des modes de distribution des lithofaciès pyroclastiques préservés dans les cônes de scories, les anneaux de tuf et les maars permet d'estimer l'ampleur de l'érosion depuis la fin de l'activité volcanique. L'étude de la population des clastes lithiques accidentels dans les roches pyroclastiques des vestiges de volcans basaltiques de type maar ou anneau de tuf dans la Zone Volcanique Waipiata (ZVV) d'âge miocène, en Nouvelle-Zélande, s'avère un bon outil pour reconstruire la stratigraphie disparue et pour estimer la valeur de l'érosion depuis la fin de l'activité volcanique. Un exemple tiré de la forme résiduelle du complexe volcanique à cratères multiples de Swinburn (ZVV), postérieurement basculé, démontre l'importance de l'effet de la prise en compte de la déformation sur les calculs de la vitesse de l'érosion. L'étude de trois événements de la ZVV suggère une gamme de taux d'érosion comprise entre 3.75 et 46 m/Ma, le résultat dépendant de 1) la position de la forme résiduelle par rapport aux blocs soulevés et 2) du fait que l'on considère ou non dans les calculs l'effet de la déformation postérieure.

Mots clés : maar, anneau de tuf, cône de scorie, érosion, Groupe Volcanique de Dunedin, Zone Volcanique de Waipiata, Nouvelle-Zélande.

Version française abrégée

L'érosion des cônes de scories, des anneaux de tuf et des maars peut être évaluée d'après la différence altitudinale entre les terrains pré-volcaniques et volcaniques et la topo-

graphie environnante, lorsque des contacts subhorizontaux peuvent être identifiés entre ces terrains et/ou lorsque des formations pyroclastiques issues de périodes de construction des appareils volcaniques aujourd'hui érodés peuvent être retrouvées sur leurs marges (tab. 1). Dans tous les autres

* Otago University, Geology Department, PO Box 56, Dunedin, New Zealand. E-mail: nemeth_karoly@hotmail.com

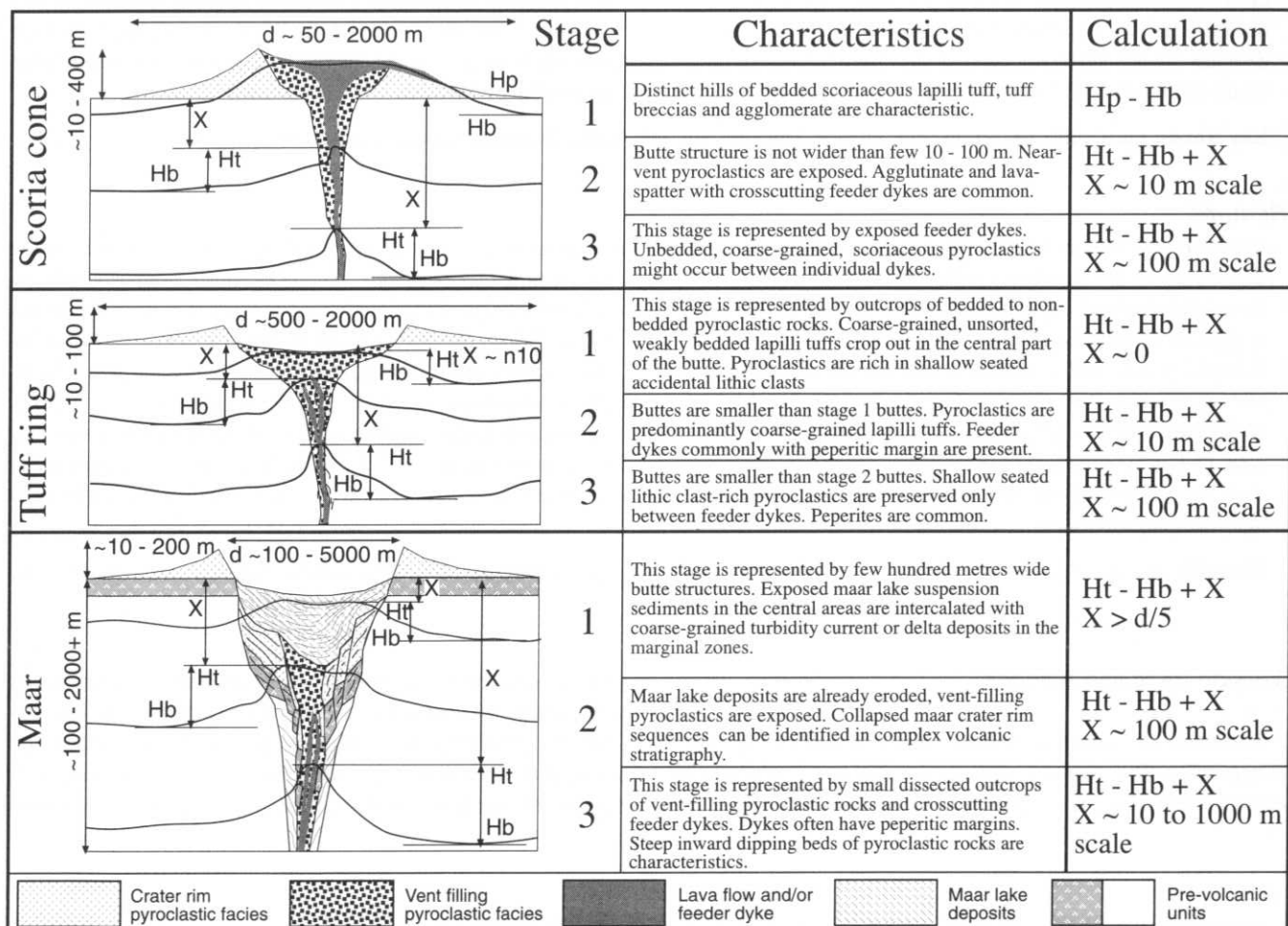
cas, là où les terrains volcaniques et pré-volcaniques ne présentent pas un contact subhorizontal et/ou les édifices volcaniques résiduels montrent des faciès pyroclastiques très proches, l'érosion peut être calculée au moyen de la différence altitudinale entre le sommet de l'appareil érodé et la topographie environnante, corrigée par un paramètre X (tab. 1). Le paramètre X est la "profondeur d'érosion", dont l'estimation repose sur l'identification de la répartition des faciès pyroclastiques sur et autour de l'édifice volcanique résiduel.

L'estimation du paramètre X dans le cas des cônes de scories est fondée sur l'identification et l'abondance de dykes d'alimentation, de "spatters" de lave clastogéniques et de dépôts centraux soudés dans les vestiges des cônes érodés. Dans le cas des anneaux de tufs, l'identification de tufs bréchiques remplissant les cratères et de dykes d'alimentation avec leurs marges péperitiques semble être essentielle pour estimer correctement le paramètre X (tab. 1). Dans le cas des maars (tab. 1), cinq critères importants permettent d'estimer correctement le paramètre X : 1) la répartition des dépôts d'écoulements pyroclastiques gravitaires, distingués des formations volcanoclastiques remaniées, 2) les dépôts lacustres formant les unités centrales, 3) les dépôts pyroclastiques très proches dans les parois effondrées ou subsidentes vers l'intérieur de l'ancien cratère, 4) les dépôts de tuf de lapilli et de brèches remplissant le cratère, et 5) la zone de la racine profonde et ses dykes d'alimentation, dont les marges sont souvent péperitiques.

Après avoir décrit les différentes étapes de l'érosion des cônes de scories, des anneaux de tuf et des maars, l'auteur présente le cas exemplaire des vestiges de différents types de volcans dans la Zone Volcanique Waipiatia (ZVW), d'âge miocène inférieur, en Nouvelle Zélande (fig. 1). Un événement (Swinburn West) situé dans un complexe volcanique de plusieurs cratères, dans la zone septentrionale de la ZVW, a été choisi pour démontrer la complexité du calcul de la vitesse de l'érosion dans les régions affectées par un basculement tectonique succédant à l'activité volcanique (fig. 2, fig. 3 et fig. 4). Les taux d'érosion calculés vont de 3.75 à 15.6 m/Ma selon que l'on prenne ou non en compte le basculement tectonique postérieur au volcanisme. Les autres cratères de la

Table 1 – Steps of erosion on terrestrial monogenetic volcanic landforms, recognition criteria, and general calculation of the erosion based on these landforms. Hp: elevation of the pre-volcanic contact; Ht: elevation of the top of the erosional remnant; Hb: background reference point elevation; X: correction value based on the recognition of stage of erosion.

Tableau 1 – Niveaux d'érosion de formes volcaniques monogéniques, critères de reconnaissance et calcul général de l'érosion fondé sur ces formes. Hp : altitude du contact pré-volcanique/volcanique ; Ht : altitude du sommet de la forme volcanique résiduelle ; Hb : altitude du point de référence en arrière-plan ; X : valeur de la correction fondée sur la reconnaissance de l'étape de l'érosion.



ZVW ont été choisis pour démontrer l'utilité de l'analyse de la population des clastes lithiques accidentels dans les roches pyroclastiques, pour qui veut reconstruire la stratigraphie pré-volcanique déjà érodée. À partir de deux localités (*The Crater*, fig. 5 ; *Black Rock*, fig. 9), des arguments plaident en faveur de la présence d'épais terrains cénozoïques durant la période de construction volcanique (fig. 7). L'évaluation de l'épaisseur des terrains cénozoïques érodés a permis de calculer un taux d'érosion de 30 m/Ma pour *The Crater* (fig. 6 et 8) et de 46 m/Ma pour *Black Rock* (fig. 9). Afin d'améliorer l'estimation de la vitesse de l'érosion en général, l'auteur fournit un modèle considérant le basculement postérieur de la zone volcanique (fig. 10 et fig. 11). D'après l'étude du cas de la zone volcanique de Waipiata, les vitesses d'érosion semblent dépendre de la position relative de l'appareil volcanique résiduel par rapport à la position des blocs environnants, plissés ou faillés et soulevés. La gamme des vitesses d'érosion obtenues est en bon accord avec les résultats de calculs fondés sur d'autres méthodes.

Introduction

Volcanic landforms of continental basaltic volcanic fields are scoria cones, tuff rings, maars and tuff cones (Fisher and Schmincke, 1984; White, 1991). This paper present a summary of long-term erosion calculations based on erosion remnants of scoria cones, tuff rings and maars to develop accurate methods for measuring the rates of geomorphic processes that shape volcanic constructs (Thouret, 1999). In this paper the term "pyroclastic" is used after the classification scheme of R. V. Fisher and H.U. Schmincke (1984, p.239). Any rock fragment expelled through a vent by volcanic explosions is a pyroclast. Pyroclast can be 1) juvenile, which includes fragments of magma involved in explosion, or 2) accidental (lithic) clasts, which record explosive disruption of pre-volcanic strata.

Long-term erosion rate is defined as the erosion of a pre-volcanic landscape "preserved" by eruptive products of small, terrestrial volcanoes, on a timescale of millions of years. Estimation of different stages of erosion of volcanoes is possible with the identification of preserved pyroclastic facies in the eroded remnants of volcanoes (Németh and Martin, 1999). Relative "erosional depth" of exposed volcanic units can then be estimated. The background elevation (H_b) is a reference elevation around the volcanic remnants. This is the elevation of the area (km-scale) surrounding the erosional remnant. The elevation of the pre-volcanic/volcanic contact is abbreviated by H_p (pre-volcanic surface elevation), and the elevation, hills capped by various rocks, by H_t. An X value is introduced to correct the calculated values of elevation difference based on measurable elevation data. Estimating X is the most critical value in the calculation of erosion rates, and possible criteria for estimation of X is given in this paper based on examples from the Miocene Waipiata Volcanic Field, South Island, New Zealand, following a brief description of the general characteristics of steps of erosion of scoria cones, tuff rings and maars.

Erosion rate calculation methods

Scoria cones

Scoria cones are the most widespread volcanic landforms on Earth (Vespermann and Schmincke, 2000). Their deposits commonly have two distinct facies: 1) a welded, coarse-grained pyroclastic and lava core zone around the vent, and 2) a distal zone (tab. 1). The core zones of scoria cones are resistant to erosion due to common welding. The erosion of the distal zone depends on climatic factors (i.e., rain-fall, e.g., White, 1991). There is an agreement that a scoria cone can completely vanish after million years (Wood, 1980; Dohrenwend *et al.*, 1986). The long-term erosion of an area based on scoria cone degradation can be established in three stages (tab. 1).

Tuff rings

Tuff rings are small volcanoes (< 100 high, < 1000 m in diameter) with a wide crater few hundred meters across and a small pyroclastic rampart (< 100 m) (Fisher and Schmincke, 1984; White, 1991; Vespermann and Schmincke, 2000) (tab. 1). Tuff rings have no deeply excavated vent zone (Lorenz, 1986). Therefore their deposits are poor in excavated accidental lithic clasts (< 25 vol%) and rich in juvenile, often vesicular glassy pyroclasts formed through magma/water interaction (Fisher and Schmincke, 1984; Sohn, 1996; Vespermann and Schmincke, 2000). Syn-volcanic collapse and small-scale slumping are possible, but is not common as in maars (Fisher and Schmincke, 1984). The transition to maar volcanoes is continuous, and long-term erosion of tuff rings could produce similar facies patterns to eroded maar remnants. The erosion stages of tuff rings and the possible calculation methods are presented on table 1.

Maar volcanoes

Maar volcanoes are low volcanic cones with bowl-shaped craters that are wide relative to rim height and cut deep into the country rock (Heiken, 1971; Fisher and Schmincke, 1984; Lorenz, 1986; White, 1991; Vespermann and Schmincke, 2000). Maars have a deeply excavated vent zone, which is filled by fall back of phreatomagmatic tephra, subsided blocks from crater rim and pre-volcanic units and lacustrine sediments (White, 1990, 1992; Büchel, 1993) (tab. 1).

The large amount (10 to 95 vol%) of accidental lithic clasts in pyroclastic rocks, a strong negative Bouguer-anomaly and a positive geomagnetic anomaly around erosion remnants imply a maar origin. Root zones of maar volcanoes can penetrate ~1500 m or more into pre-volcanic units (Lorenz, 1986, 2000a,b). The complex vent/conduit zone (diatreme) is filled by collapsed pyroclastic units, explosion breccias and large subsided pre-volcanic units in a chaotic situation (Lorenz *et al.*, 1970; Lorenz, 2000a,b). Typical maar crater have a diameter to depth ratio of 1 to 5, but this figure is only loosely constrained (Mertes, 1983; Lorenz,

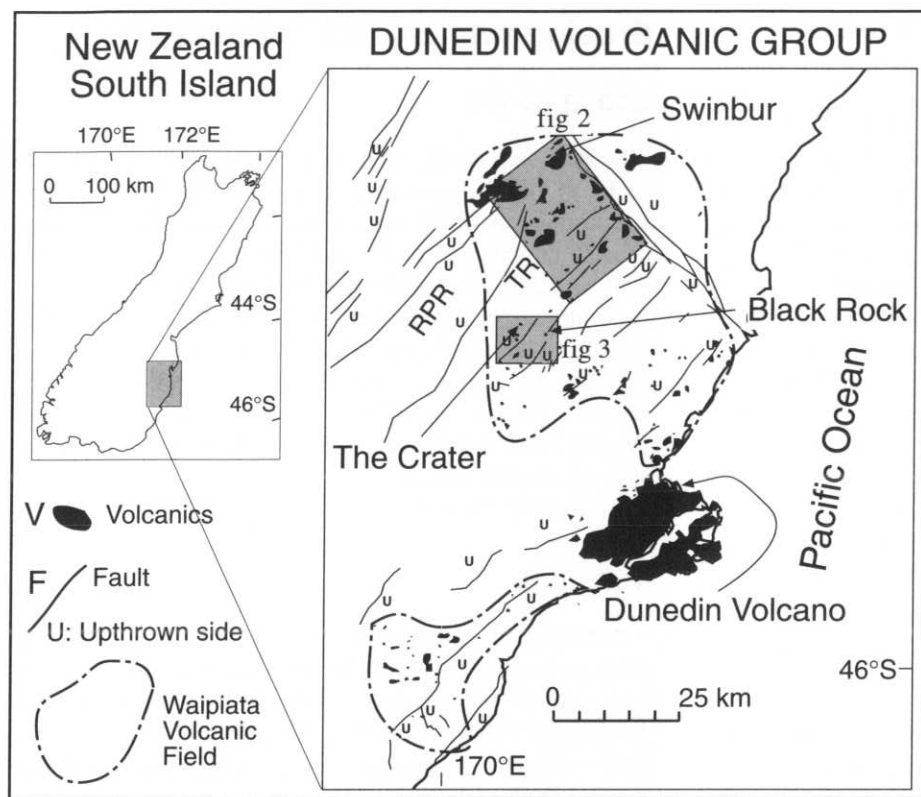


Fig. 1 – Vent remnants of the Waipiata Volcanic Field, part of the Dunedin Volcanic Group. Studied vents are marked. Shaded areas represent part of the field presented on detailed topographic maps on fig. 2 and 3. RPR: Rock and Pillar ridge; TR: Taieri ridge.

Fig. 1 – Vestiges des cratères de la Zone Volcanique de Waipiata, partie du Groupe volcanique de Dunedin. Les événements étudiés sont indiqués. Les zones ombrées représentent une partie du terrain sur les cartes topographiques détaillées, fig. 2 et fig. 3. RPR : crête de Rock et Pillar; TR : crête de Taieri ; V : formations volcaniques ; F : faille ; U : bloc soulevé par la faille.

followed Late Cretaceous extension and separation of New Zealand from Gondwana (Carter, 1988) causing widespread marine clastic sedimentation in the area (Oligocene marine sequences - OMS). These marine units are generally fine sandstones, siltsstones with variable amount of glauconite. In the northern part of

the Waipiata Volcanic Field, limestone beds are developed above marine clastic units (Green Valley Limestone - GL). The area re-emerged in the early Miocene in response to transpressional tectonics with the inception of the Alpine Fault (Cooper *et al.*, 1987). This period is marked by terrestrial fluvio-lacustrine clastic deposition (Dunstan Formation - DF). Late Miocene - Pliocene uplift of ranges on the north side of the schist belt initiated deposition of extensive fan-globularites and braidplain deposits to the south of these newly emerged ranges (Wedderburn Formation - WF). These deposits grade upward into a more voluminous, immature, greywacke-dominated conglomerate. The youngest terrestrial sediments are named Maniototo Conglomerate in the northern side of the WVF (Youngson *et al.*, 1998).

Erosion remnants of scoria cones, tuff rings and maars of WVF form a characteristic landscape with volcanic buttes (figs. 2 and 3). Cenozoic sedimentary units are preserved predominantly in the northern margin of the WVF partly due to thick lava flows (fig. 2). In the central, uplifted fault/fold block areas of the WVF Cenozoic sedimentary units are not preserved, and the only information on their existence or non-existence may be derived from the pyroclastic deposits preserved in various volcanic pipes (fig. 3) which highlights the importance of studying volcanic fields like the Waipiata Volcanic Field. In the following sections case studies will be presented from the WVF.

Swinburn

Swinburn Volcanic Complex is located in the northern margin of the WVF (figs. 1 and 2) and is a special combination of eroded (stage 2 erosion) scoria cones and

1986). The largest known maar volcano is ~5000 m in diameter (Beget *et al.*, 1996) and the smallest is less than 100 m (Schmincke, 1977; Fisher and Schmincke, 1984). The depth of excavation is in the same range as the crater diameter (Lorenz, 1986), but it may be significantly larger in "accidental lithic-rich" maars (Gevrek and Kazancı, 2000; Németh *et al.*, 2000).

The amount of erosion in each erosion stage is calculated from the elevation difference between the top of remnant and the background elevation, corrected with an X value (tab. 1). The difference between erosion calculation based on scoria cones, tuff rings and maars is that maars are negative landforms in contrast to scoria cones and tuff rings which are constructive landforms. In this respect, maars function as sedimentary basins, and pyroclastic rocks preserved in maars and exhumed after erosion represent rocks deposited originally below the paleosurface (tab. 1).

Examples from New Zealand

Geological setting

The eroded volcanoes considered here (fig. 1) belong to the Early Miocene Dunedin Volcanic Group (DVG) (Coombs and Reay, 1986) and form the Waipiata Volcanic Field (WVF) (Németh, 2001). The pre-volcanic Cenozoic units consist of non-marine and marine clastic sediments (Youngson and Craw, 1996) deposited on an early Cretaceous erosional surface (LeMasurier and Landis, 1996) cut into a schist basement (Otago Schist - OS). The oldest terrestrial clastic sediments deposited on the schist form the Hogburn Formation (HF). Marine transgression

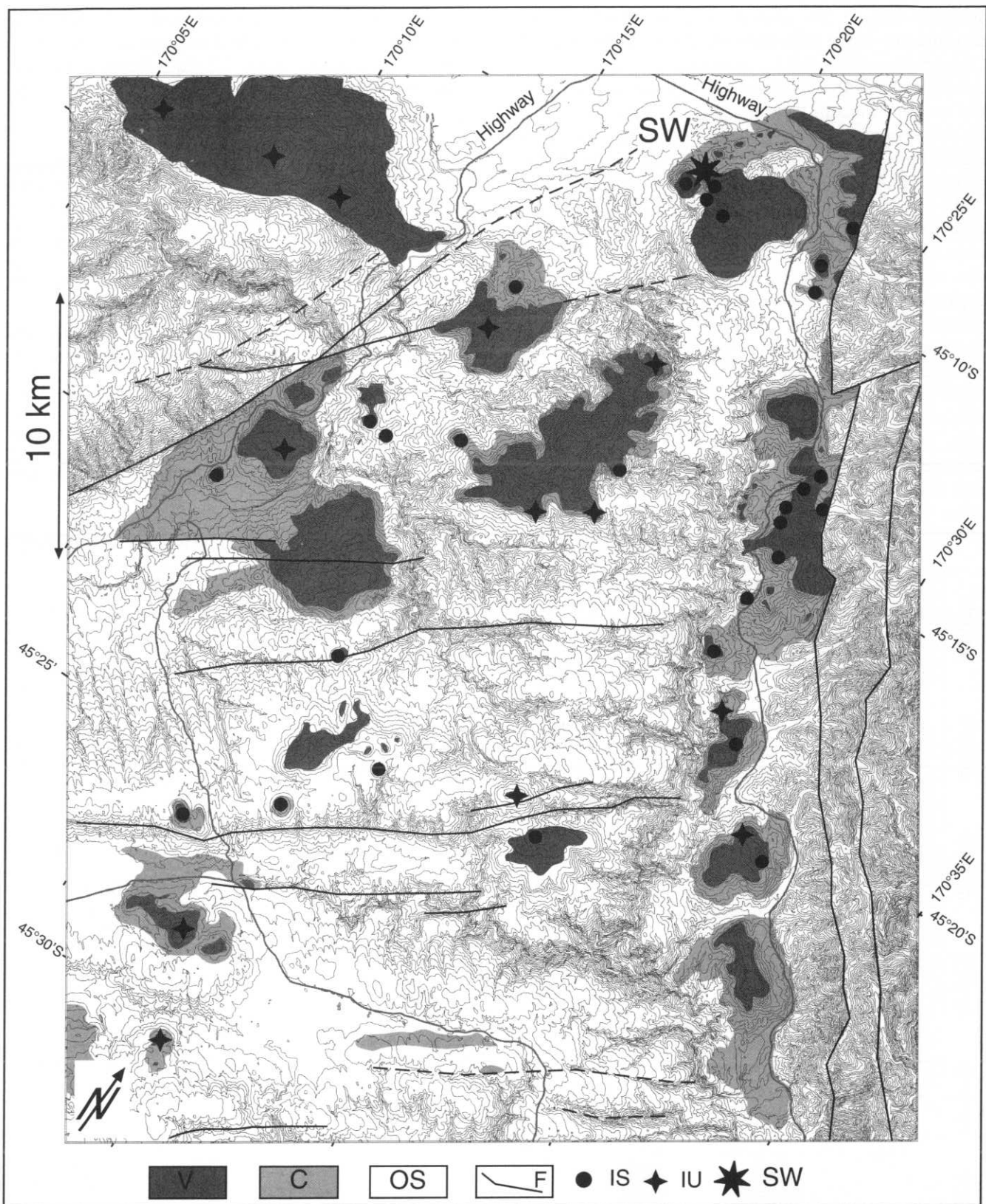


Fig. 2 – Geomorphology of the northern part of the Waipiata Volcanic Field (topographic contours at 20 m intervals). Note the preserved Cenozoic units nearby the volcanic erosional remnants. V: volcanics; C: Cenozoic units; OS: Otago Schist; F: fault; IS: inferred position of vents, sure; IU: inferred position of vents, unsure; SW: location of Swinburn west vent.

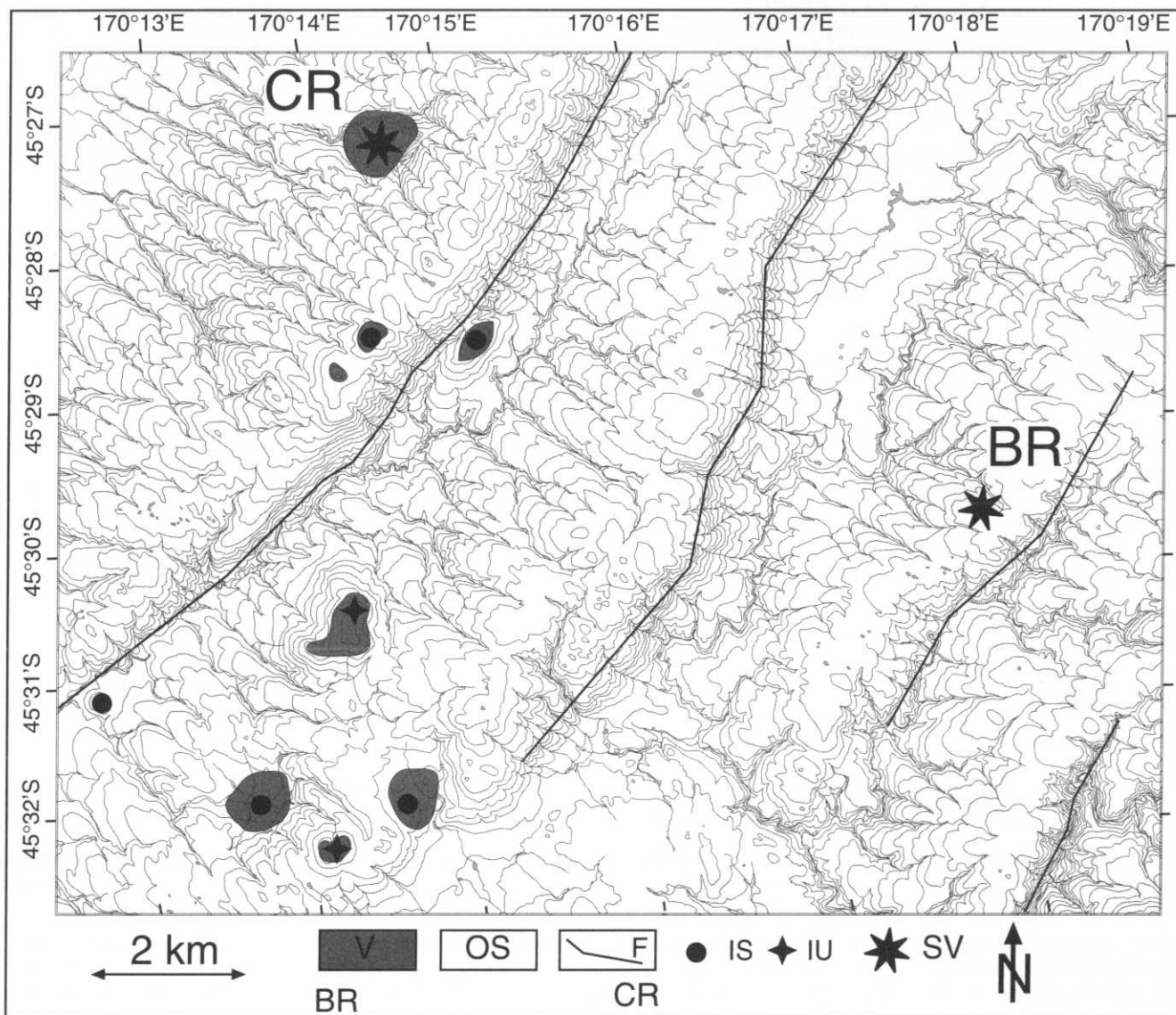
Fig. 2 – Géomorphologie de la partie septentrionale de la Zone Volcanique de Waipiata (équidistance des courbes de niveau : 20 m). Noter les terrains cénozoïques préservés près des vestiges des édifices volcaniques. V : terrains volcaniques ; C : terrains cénozoïques ; OS : schistes d'Otago ; F : faille ; IS : position probable des événements, sûre ; IU : position probable des événements, incertaine ; SW : localisation du cratère ouest de Swinburn.

diatremes (tab. 1). The studied site is an eroded maar/tuff ring filled by scoria cone deposits. The Swinburn Volcanic Complex is accompanied by an extensive basaltic lava plateau (figs. 2 and 4). The area covered by lava is at least ~10 km² on the Swinburn Plateau and the average elevation of the flat lava-capped hills is ~650 m (figs. 2 and 4). The exposed pre-volcanic units consist of Otago Schist overlain by units HF, OMS and GL. Along the northwestern margin of the lava field at least five vents are identified, each with an initial phreatomagmatic pyroclastic unit (fig. 4). Three vents have no magmatic explosive capping unit. The other two remnants are predominantly products of magmatic explosive eruptions. The general westward dip of the pre-volcanic units suggests a possible subsequent tilting and/or steep pre-volcanic paleoslopes in the region (fig. 4). The example vent is a 200-300-m-wide remnant of a scoriaceous lapilli tuff and agglomerate butte which cuts through a pre-volcanic unit of OS, HF, OMS beds with steep contacts (figs. 4 and 5). The lower few meters of the pyroclastic sequence consists of strongly palagonitised sideromelan-rich bedded lapilli tuff and tuff beds. The majority of

pyroclastic rocks are coarse-grained, weakly to non-bedded scoriaceous lapilli tuff, or welded scoriaceous agglomerate. On the highest point of the hill-side, feeder dykes cut through the pyroclastic units and gradually transform into major eastward directed lava flows (fig. 4).

Fig. 3 – Geomorphology of the central part of the Waipiata Volcanic Field (topographic contours at 20 m intervals). Note that there is no preserved Cenozoic unit in this part of the volcanic field, erosion having cut back to the level of the basement Otago Schist. Also note the northwestward dipping fault/fold blocks. V: volcanics; OS: Otago Schist; IS: inferred position of vents, sure; IU: inferred position of vents, unsure; F: fault; SV: studied vents, Black Rock (BR) and "The Crater" (CR).

Fig. 3 – Géomorphologie de la partie centrale du Waipiata Volcanic Field (équidistance des courbes de niveau : 20 m). Noter l'absence de terrains cénozoïques préservés dans ce secteur volcanique, l'érosion ayant agi jusqu'au niveau des schistes d'Otago du substratum. Noter également les blocs inclinés vers le nord-ouest. V : terrains volcaniques ; OS : terrains cénozoïques ; OS : schistes d'Otago ; IS : position probable des événements, sûre ; IU : position probable des événements, incertaine ; F : faille ; SV : cratères étudiés, Black Rock (BR) et "The Crater" (CR).



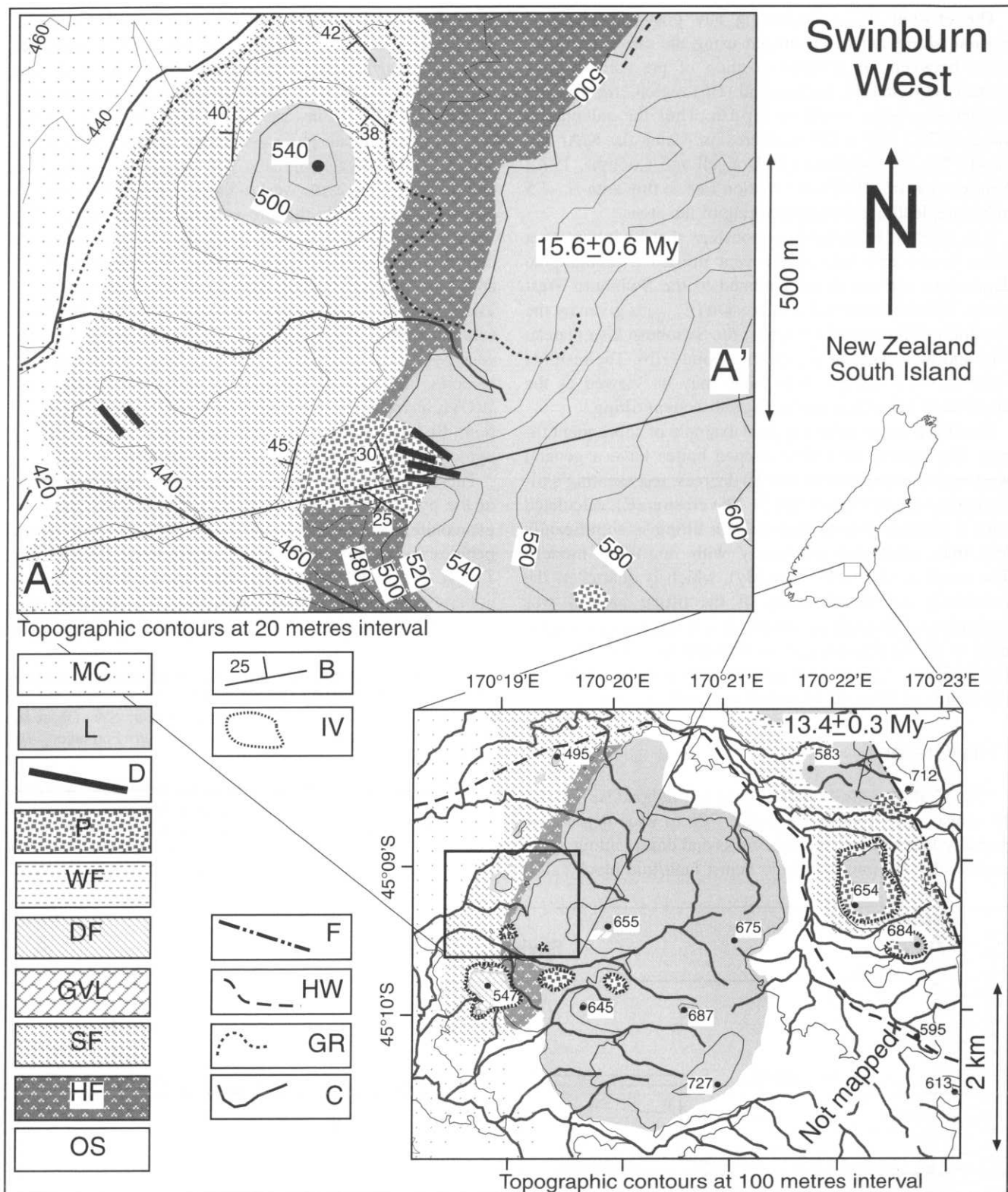


Fig. 4 – Geology map of the Swinburn west area. AA': cross section shown on fig. 5. MC: Maniototo conglomerate (Pliocene-Quaternary); L: lava flow (Miocene); D: dyke; P: pyroclastic rocks (Miocene); WF: Wedderburn Formation (Miocene); DF: Dunstan Formation (Miocene); GVL: Green Valley Limestone (Oligocene); SF: marine sequence (Swinburn Formation, Oligocene); HF: Hogburn Formation (Eocene); OS: Otago Schist (Cretaceous); B: bedding with dip azimuth; IV: inferred position of vents; F: Fault; HW: Highway; GR: Gravel road; C: Creek. Elevations are in meters.

Fig. 4 – Carte géologique de la zone ouest de Swinburn. AA' : coupe de la fig. 5. MC : congolomérats de Maniototo (Pliocène -Quaternaire) ; L : coulée de lave (Miocène) ; D : dyke ; P : roches pyroclastiques (Miocène) ; WF : formation Wedderburn (Miocène) ; DF : formation Dunstan (Miocène) ; GVL : calcaires de Green Valley (Oligocène) ; SF : séquence marine (formation Swinburn, Oligocène) ; HF : formation Hogburn (Eocène) ; OS : schistes d'Otago (Crétacé) ; B : stratification avec azimuth du pendage ; IV : position probable des événements ; F : faille ; HW : route principale ; GR : piste ; C : ruisseau. Altitudes en mètres.

The erosion (E_{\max}) neglecting any post-volcanic/post-erosion tilting can be calculated using the elevation difference between the inferred position of pre-volcanic/lava contact (H_p) and the background (H_b) region (fig. 5). The calculated erosion would be $H_p - H_b$. Thus the calculation yields $\sim 530 - 410 = 120$ m of erosion. Using the K/Ar age of ~ 16 My for Swinburn (McDougall and Coombs, 1973; Youngson *et al.*, 1998), the erosion rate in this area is ~ 7.5 m/My neglecting subsequent tilting of the area.

It is inferred from field relationships that Swinburn lava flows in the east side of the vent infilled a topographic depression and are directly related to the Swinburn West vents. The maximum value of erosion ($E_{\max 2}$) is given by the elevation difference of the top of the Swinburn lava plateau (H_t) and the background reference point (H_b). The result is ~ 250 m (15.6 m/My). This value may be viewed as the upper limit of erosion neglecting subsequent tilting.

Swinburn seems to be a typical example of subsequent tilting. The nearby lava flow capped buttes have a general westward dip direction of 5 to 10 degrees, representing a tilted paleo-surface (figs. 4 and 5). The erosion (E), calculated with 5 degrees general post-erosion tilting is significantly less than calculated previously with non-tilted models. The result is ~ 60 m (3.75 m/My), which is quarter of the previously calculated values. If the tilting process was "continuous" throughout ~ 16 My, it is a reasonable compromise to fix the possible erosion between these two numbers (60 - 250 m; 3.75 to 15.6 m/My). The realistic erosion in the area is ~ 150 m, or 10 meters per million years.

"The Crater"

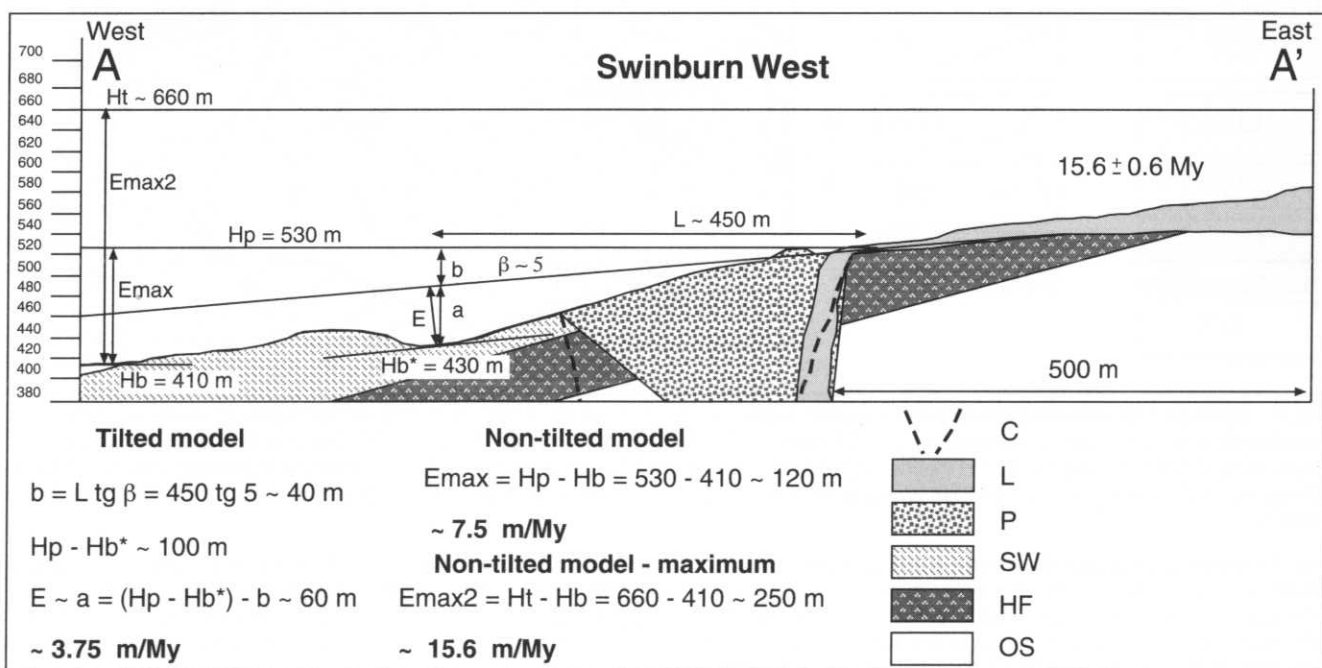
"The Crater", named for its circular tuff rampart surrounded by schist, is a ~ 1000 m long and ~ 700 m wide depression, partially filled with pyroclastic rocks and cross-cutting dykes and/or sills, cut into the Otago Schist fault/fold block called

Taieri Ridge (figs. 3 and 6). In the vicinity (10 km scale) of The Crater, there is no Cenozoic pre-volcanic rock preserved (fig. 3). The pyroclastic rocks of The Crater can be divided into 2 major units. Unit 1 (collapsed bedded crater rim unit - CBCR) is a series of inward dipping beds recording deposition from near-vent phreatomagmatic pyroclastic density currents, and phreatomagmatic and magmatic fallout. This unit occurs mainly in the west of the area and shows a steeply dipping contact with the pre-volcanic Otago Schist. Dip values of inward dipping beds gradually increase toward the pre-volcanic/volcanic contact, reaching 65-75 degrees. Unit 2 consists of pyroclastic beds that occur in the central area of The Crater and is subdivided into two sub-units. The basal sub-unit (lithic-rich central unit - LRU) consists of non- or weakly-bedded accidental lithic-rich lapilli tuffs and tuff breccias. The capping sub-unit (juvenile-rich central unit - JRU) is increasingly rich in sideromelane glass shards up-section. Bedding planes are well developed in the capping pyroclastic sequences, and dip radially inward.

The composition of the accidental lithic-clast population of the pyroclastic rocks at The Crater varies but abundant glauconite is inferred to derive from OMS units, and quartz pebbles present are characteristic of HF units. Beds of unit 1 have previously been interpreted as a complex inward collapsed former crater rim sequence of a maar volcano (Németh, 2000). Beds of unit 2 have been interpreted as the

Fig. 5 – Cross-section of the Swinburn west vent and the possible ways of calculating the erosion rate. C: non-tilted volcanic conduit wall; L: lava flow; P: pyroclastic rocks; SW: Oligocene marine; SW: Swinburn Formation; HF: Hogburn Formation; OS: Otago Schist.

Fig. 5 – Coupe de l'évent ouest de Swinburn et méthodes envisageables pour les calculs des vitesses d'érosion. C : paroi de la cheminée volcanique non basculée ; L : coulée de lave ; P : roches pyroclastiques ; SW : sédiments marins d'âge oligocène ; SW : formation Swinburn ; HF : formation Hogburn ; OS : schistes d'Otago.



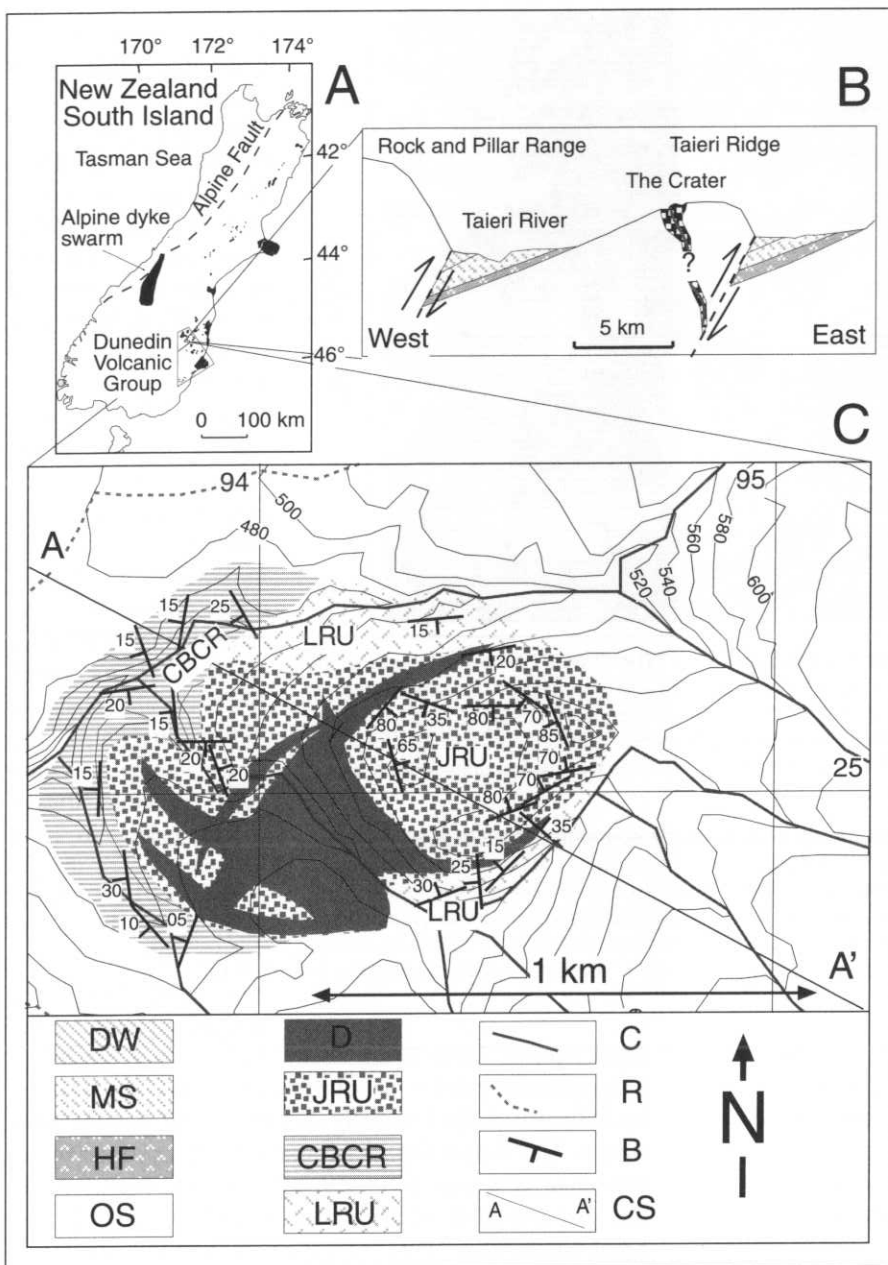


Fig. 6 – Simplified geology map of "The Crater". Cross-section on B is simplified showing major relationships between uplifted fault/fold blocks, location of Cenozoic sediments and volcanic pipes. OS: Otago Schist; HF: Hogburn Formation; MS: Oligocene marine sequences; DW: Dunstan and/or Wedderburn Formation; LRU: lithic-rich pyroclastic unit; CBRC: collapsed, bedded crater rim pyroclastic unit; JRU: juvenile-rich pyroclastic unit; D: dykes; CS: cross-section on fig. 8; B: bedding; R: gravel road; C: creek.

Fig. 6 – Carte géologique simplifiée du "Cratère". La coupe en B, simplifiée, montre les relations majeures entre les blocs soulevés, la position des sédiments cénozoïques et les cheminées volcaniques. OS : schistes d'Otago ; HF : formation Hogburn ; MS : sédiments marins d'âge oligocène ; DW : formation Dunstan et/ou Wedderburn ; LRU : unité pyroclastique riche en lithiques ; CBRC : unité pyroclastique stratifiée de la paroi du cratère effondrée ; JRU : unité pyroclastique riche en juvéniles ; D : dykes ; CS : coupe sur la fig. 8 ; B : pendage ; R : piste ; C : ruisseau.

central part of a conduit filling pyroclastic facies (basal unit) with later inward collapsed crater rim (capping unit) beds (Németh, 2000).

The Crater shows morphology characteristic of advanced, stage 2 erosion of a phreatomagmatic, possible maar volcano. Maar lake-beds are lacking and large inward subsided blocks of former crater rim beds are exposed. The size of The Crater allows a reconstruction of an approximately 1000-m-wide maar crater. This suggests a crater-depth of 200 m (Lorenz, 1986) which implies that the present exposure is at least 200 m below the syn-volcanic paleosurface. The present exposure is well below this level, because pyroclastic rocks of The Crater contain accidental lithic clasts derived from pre-volcanic units already eroded at The Crater. Clasts like sandstone or glauconite (fig. 7) characteristic of Oligocene marine (OMS) units, or small pebbles typical of Early Eocene Hogburn Formation (HF), indicate that these sedimentary units must have been present during

eruption and were subsequently cut through by "The Crater" vent. Calculation of erosion rates requires estimation of the possible thickness of already eroded Cenozoic units (HF, OMS, DF). The maximum possible thickness of unit HF is approximately 100 m. Unit OMS was not more than 200 m thick in this region based on field relationships to other areas, where these Cenozoic units are preserved (J. Youngson, pers. com., 2000). This implies that at least 300 m of Cenozoic sedimentary strata have

been eroded away. With a maximum of 100 m erosion of the schist surface an erosion depth of 400 m is inferred (fig. 8). There is no available age data yet from this locality, thus an average age of 12 million years is estimated based on K/Ar age data for the Dunedin Volcanic Group (Coombs and Reay, 1986). Calculating the total erosion rate using this age implies an erosion rate of ~30 m/My.

Black Rock

Black Rock is a pyroclastic rock capped small butte on the Otago Schist (figs. 3 and 9). There are no preserved Cenozoic pre-volcanic units in the vicinity of the pyroclastic rocks at Black Rock (figs. 3 and 9). The pyroclastic butte is approximately 20 m above the steep contact zone of the pre-volcanic/volcanic units. The pyroclastic butte is semi-circular with a diameter <200 m. Pyroclastic rocks at Black Rock consist of very uniform, unsorted, non- or weakly

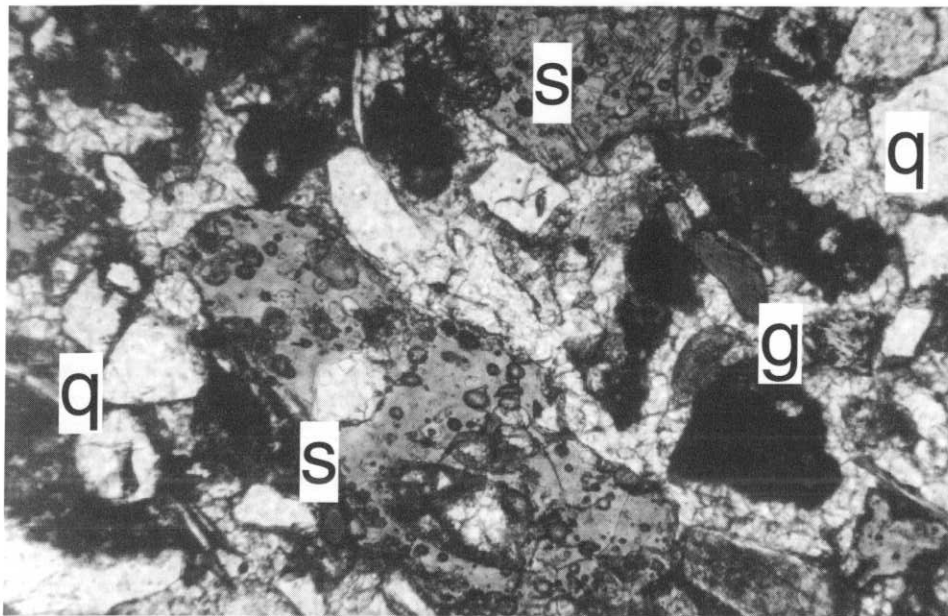


Fig. 7 – Photomicrograph of a lapilli tuff from the top section of "The Crater". Note the sideromelane shards (s) formed by magma/water interaction of rising tephritic magma and groundwater. The angular quartz shards must have been derived from Otago Schist (q) in contrast to rounded quartz pebbles which are inferred to be derived from Eocene Hogburn Formation. Glauconite (g) is incorporated into pyroclastic rocks from Oligocene marine units, and their presence in the pyroclastic rocks indicates that marine units formed part of the pre-volcanic sequence during volcanism.

Fig. 7 – Photographie de lame mince d'un tuf de lapilli de la partie sommitale du "Cratère". Noter les échardes de sidéromélane (s) formées par l'interaction hydromagmatique d'un magma téphritique ascendant avec la nappe phréatique. Les échardes angulaires de quartz doivent provenir des schistes d'Otago (q), contrairement aux quartz arrondis qui seraient issus de la formation éocène d'Hogburn. De la glauconite (g) des sédiments marins oligocènes est incorporée aux roches pyroclastiques ; leur présence dans les roches pyroclastiques indique que ces sédiments marins formaient une partie de la séquence pré-volcanique lors de l'activité volcanique.

bedded lapilli tuff and tuff breccia, rich in sideromelane glass shards. Accidental lithic clasts range from 2.5 m long schist clasts to small metamorphic quartz aggregates derived from the Otago Schist. The pyroclastic rocks are rich in rounded millimeter-size glauconite derived from unit OMS. Occasional pebbles up to 5 mm in diameter are inferred to derive from unit HF based on their morphology (Youngson and Craw, 1996; Youngson *et al.*, 1998). The pyroclastic unit is interpreted as a conduit-filling root zone of a former maar volcano based on features such as: 1) the uniform unsorted, non-bedded characteristics; 2) the semicircular distribution, and; 3) the high proportion of accidental lithic clasts (25 to 70 vol %) in the pyroclastic rocks. The diameter of the butte suggests that the recently exposed area is a deep region of a volcanic conduit formerly associated with a phreatomagmatic, possible maar volcano. The presence of large amount of glauconite in the pyroclastic rocks along with finely dispersed quartz grains indicate that a thick marine sequence (OMS) must have existed and have been cut through by the volcanic conduit. The presence of unit HF during volcanism is also supported by the occurrence of pebbles characteristic of HF units in pyroclastic rocks.

Black Rock represents stage 3 erosion of a maar (or tuff ring) volcano, based on the presence of accidental lithic rich, uniform pyroclastic rocks, the small diameter of the butte (<200 m), and sharp, steep contacts between pyroclastic and pre-volcanic units. The presence of similar accidental lithic clast populations to pyroclastic rocks from The Crater indicates that Cenozoic units must have existed and have been cut through by the Black Rock vent similarly to The Crater. Because there is no direct method to calculate the possible thickness of the already eroded Cenozoic units (Németh, 2001), thickness values of Cenozoic units similar to those estimated for The Crater are inferred for Black Rock on the basis of field relationships. The Crater is a significantly larger structure, thus it is reasonable to infer that the smaller diameter of the Black Rock represents either: 1) deeper exposure of a pyroclastic rock filled volcanic conduit than

The Crater or; 2) the Black Rock is an erosional remnant of a significantly smaller maar/tuff ring volcano than The Crater. If the Black Rock initially (before erosion) had the same size as The Crater, the recent exposure must represent an erosion level at least 100 - 150 m deeper than The Crater. In this case a total of >550 m erosion can be implied for the Black Rock butte. There is no age data from this site, therefore a standard 12 million years of age (Coombs and Reay, 1986) is used for the determination of erosion rate, which is around 46 m/My at Black Rock.

Discussion: effects of subsequent tilting on the calculation of the erosion

The previously presented examples indicate that tilting of terrestrial volcanic landforms should be considered in erosion rate calculations. Those models introduced earlier (tab. 1) apply only if there is evidence that tilting following volcanism did not occur. The problem with tilting is that the elevation data compiled from topographic maps refer to a horizontal base level, but the erosion before tilting relates to a "paleo-horizontal" level, which is now tilted. This affects: 1) positioning of the background elevation (H_b), from which point the erosion will be calculated, and; 2) the position of the paleo-surface (H_p) or top elevation (H_t) estimated from the distribution of identified volcanic units of the erosional remnant (figs. 10 and 11).

The background elevation can be calibrated by tilting back the area to its original position (figs. 10 and 11). The easiest way to approach this problem is a simple graphical method from cross-sections of the studied area. The constructed background reference-point is the point where the oldest pre-volcanic units are exposed in the vicinity of the erosional remnant (fig. 11). A line represents the horizontal distance L between the marked "erosional remnant paleo-surface" point and the point marked as a background elevation reference point (fig. 10). The erosion (E) is approximately the recent topographic elevation difference between "background" (H_b) and "erosional remnant paleo-surface" (H_p) reference point reduced by $L * \tan \beta$ where β is the estimated tilting angle (fig. 11). The value of erosion (E) calculated in this way is half to a third of the value ($E_{max} = H_p - H_b$ or $E_{max2} = H_t - H_b$) calculated without considering the tilting effect (non-tilting model) (figs. 10 and 11). It is suggested to make erosion calculations in both ways, because the true value may range between E and E_{max2} .

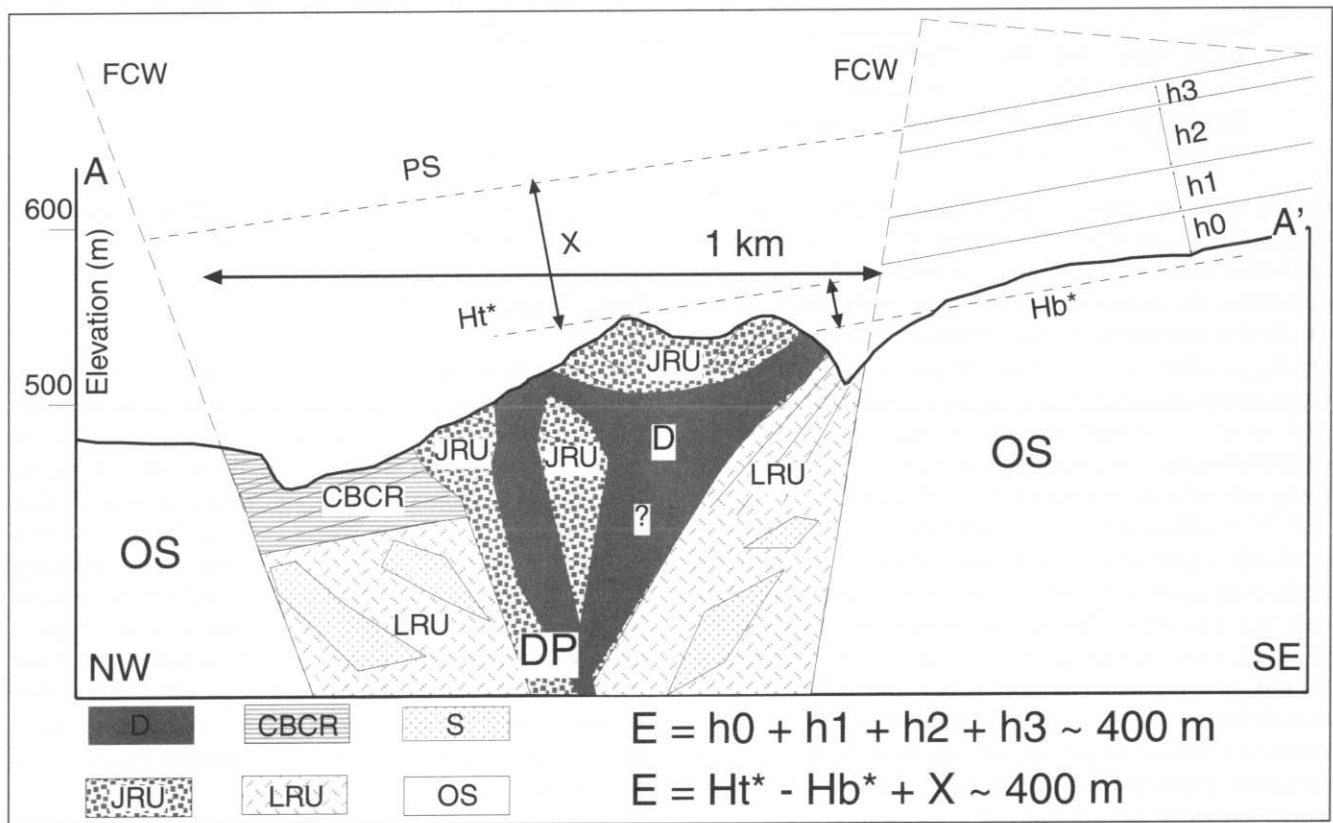
In summary, three different models can be applied to calculate erosion of a region based on remnants of terrestrial volcanic landforms according to their relationship to large-scale tilting of a region.

1) 1st model (non-tilted model). In this model a simple elevation difference between a chosen background reference point and the top of the erosion remnant of the volcano is applied to calculate the erosion (E_{max} or E_{max2}) (fig. 10). In this model, the position of the volcano is assumed to be original (non-tilted). To calculate the exact value of the erosion, the previously discussed method and estimation of X values are suggested (tab. 1).

2) 2nd model (syn- or slight post-volcanic tilting model). If the tilting occurred immediately after volcanism, the erosion is "destroying" an already tilted area and erosion proceeds according to the erosion resistance of the rocks (fig. 11). The initial erosion (E_i) which occurred while the area was horizontal should be significantly smaller than the total value of erosion (E_t close to zero). The elevation difference between

Fig. 8 – Cross-section of "The Crater" diatreme, showing identified pyroclastic units. h_0 : estimated thickness of eroded schist; h_1 : estimated thickness of eroded Hogburn Formation; h_2 : estimated thickness of eroded marine units; h_3 : estimated thickness of post-marine terrestrial units such as Dunstan Formation; H_t^* : top elevation of the erosional remnant compared to a tilted paleosurface (PS) reference line; H_b^* : background reference point elevation compared to a tilted paleosurface reference line; X : thickness of "missing units". OS: Otago Schist; LRU: lithic-rich pyroclastic unit; CBRC: collapsed, bedded crater rim pyroclastic unit; JRU: juvenile-rich pyroclastic unit; D: dykes; S: collapsed and slide in sandstone blocks; FCW: former volcanic conduit wall; DP: diatreme pipe.

Fig. 8 – Coupe du diatème du "Cratère", montrant les unités pyroclastiques identifiées. h_0 : épaisseur estimée des schistes érodés ; h_1 : épaisseur estimée de la formation Hogburn érodée ; h_2 : épaisseur estimée des sédiments marins érodés ; h_3 : épaisseur estimée des terrains continentaux tels que la formation Dunstan ; H_t^* : hauteur maximale de la forme résiduelle par rapport à la ligne de référence d'une paléo-surface inclinée ; H_b^* : hauteur d'un point de référence en arrière-plan comparée à la ligne de référence d'une paléo-surface inclinée ; X : épaisseur des "unités manquantes". OS : schistes d'Otago ; LRU : unité pyroclastique riche en lithiques ; CBRC : unité pyroclastique stratifiée de la paroi du cratère effondrée ; JRU : unité pyroclastique riche en juvéniles ; D : dykes ; S : effondrement et glissement dans des blocs de grès ; FCW : paroi de l'ancienne cheminée volcanique ; DP : cheminée de diatème.



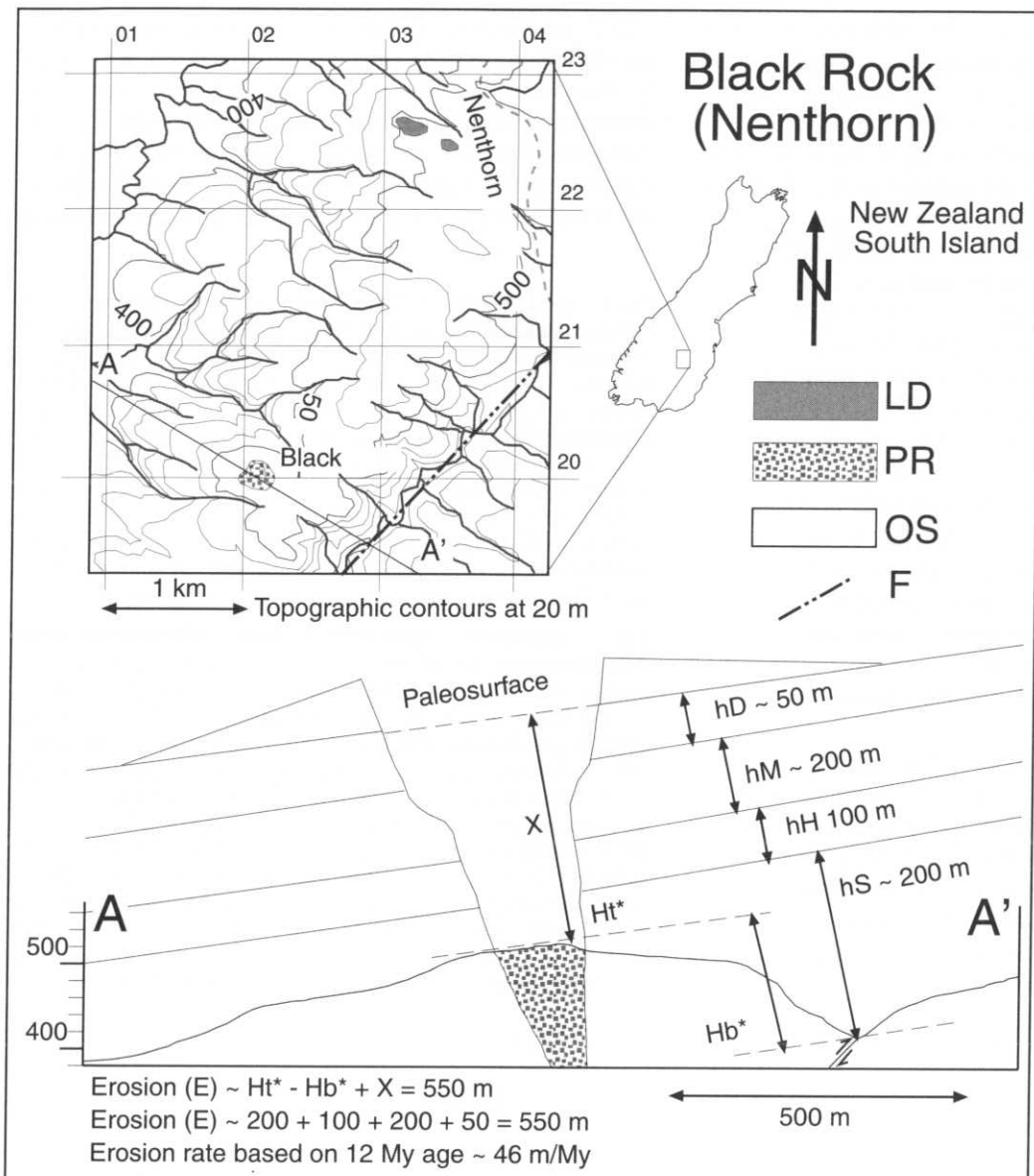


Fig. 9 – Simplified geological map and cross-section of the Black Rock diatreme. Compare with fig 8. OS: Otago Schist; PR: pyroclastic rocks; LD: lava flows or dykes; hS: thickness of eroded Otago Schist; hH: thickness of eroded Hogburn Formation; hM: thickness of eroded marine units; hD: thickness of eroded Dunstan and/or Wedderburn Formations.

Fig. 9 – Carte géologique simplifiée et coupe du diatème de Black Rock. Comparer avec la fig. 8. OS : schistes d'Otago ; PR : roches pyroclastiques ; LD : coulées de lave ou dykes ; hS : épaisseur des schistes d'Otago érodés ; hH : épaisseur de la formation Hogburn érodée ; hM : épaisseur des sédiments marins érodés ; hD : épaisseur des formations Dunstan et/ou Wedderburn érodées.

the top of the capping volcanic rocks and the background (E_{\max} and $E_{\max 2}$) in this type of tilting does not represent the real value of erosion because a significant part of the elevation difference was generated during the tilting (figs. 10 and 11). In this case the only clue to estimate erosion is the E_{\max} and $E_{\max 2}$ values, which almost certainly greatly exceed the real value of erosion. It is a reasonable estimate that the erosion in the 2nd model is close to the value of erosion calculated with the assumption that the tilting occurred relatively late after the volcanism (figs. 10 and 11).

3) 3rd model (post-volcanic tilting model). If the tilting is relatively young compared to the volcanism, the area was positioned horizontally relative to erosion most of the time (fig. 11). The tilting changed the position of the paleo-horizontal recently, thus the position of both the background and the erosional remnant reference points "moved". The elevation difference between the background and the erosional remnant reference points (E_{\max}) became greater than the elevation difference generated clearly by the erosion (E). This increase is not related to the erosion, instead it is a

result of the tilting. If any tilting is detected in the field, the third model should be used to calculate the erosion.

Conclusion

Studying erosional remnants of scoria cones, tuff rings and maars is useful for paleogeographical reconstruction. Erosion of these volcanoes follows general stages. Scoria cones are constructional landforms, in contrast to maars, which are local sediment traps. Tuff rings often represent a transitional form between scoria cones and maars from a geomorphic point of view. Scoria cones are relatively quickly degraded on a geological time scale (few hundred thousand years) and erosion leaves only a welded scoriaeous pile of pyroclastic rock or lava flows. Rim beds of tuff rings and maars can be eroded as fast as scoria cones unless they are capped by lava flows. Only the root zone of maars and tuff rings is preserved after a few million years of erosion. In this late stage of erosion it is generally hard to distinguish erosional remnants of tuff rings and maars. The

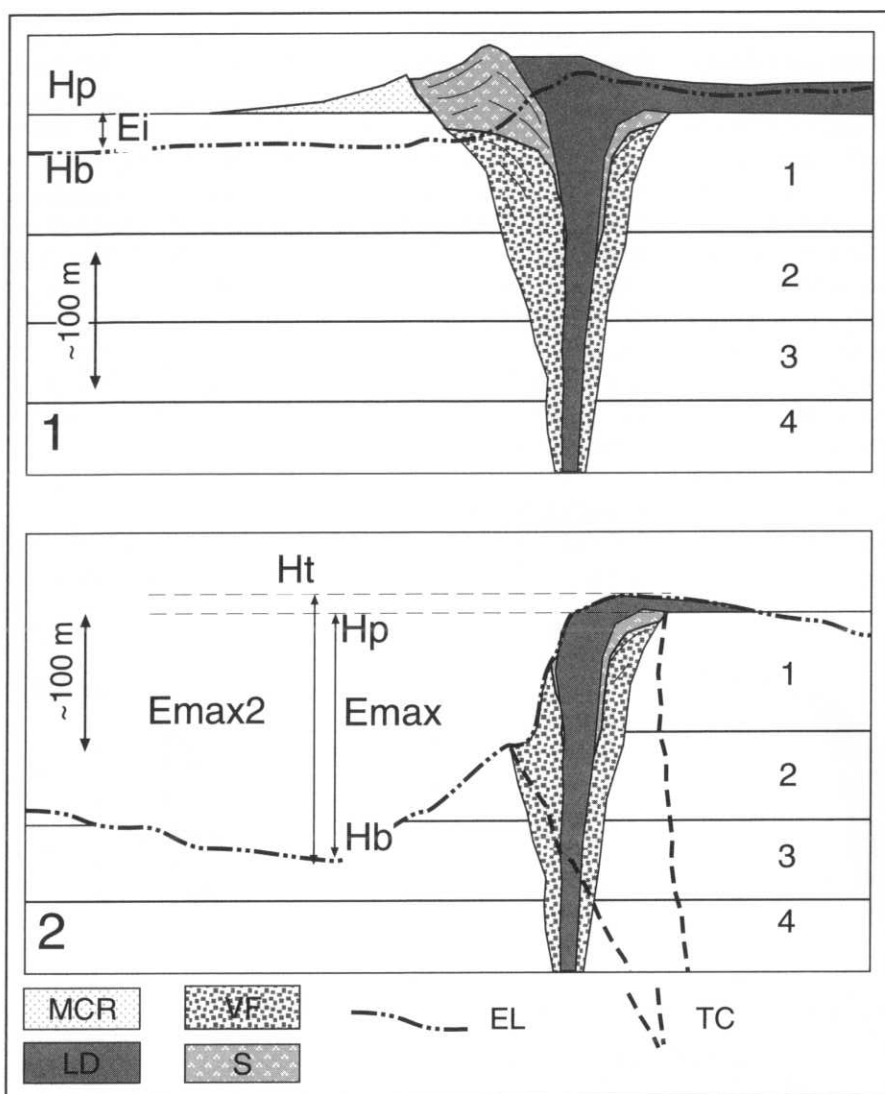


Fig. 10 – Steps in calculating erosion on lava-capped scoria cones with phreatomagmatic base. Non-tilted model, no subsequent tilting is estimated. 1: **initial erosion stage.** Hp: elevation of pre-volcanic/volcanic contact; Hb: elevation of background reference point; Ei: initial erosion. 2: **advanced stage of erosion.** Ht: elevation of the top of the lava capped butte; Hp: elevation of pre-volcanic/volcanic contact (paleosurface); Emax is an erosion calculated to the estimated position of the pre-volcanic/volcanic contact (paleosurface); Emax2 is an erosion calculated while assuming that the top of the sequence marks the paleosurface (e.g., crater-filling lava lake). Numbers 1, 2, 3, 4 represent pre-volcanic rock units. LD: lava flows and/or dykes; MCR: pyroclastic beds of maar/tuff ring crater rim; S: scoria beds; VF: vent filling pyroclastic units; EL: erosion line; TC: tilted contour of volcanic conduit.

Fig. 10 – Étapes des méthodes de calcul de l'érosion sur des cônes de scories recouverts de lave avec une base phréatomagmatique. Modèle non-basculé, aucune déformation postérieure n'est envisagée. 1 : **période d'érosion initiale.** Hp : hauteur du contact pré-volcanique/volcanique ; Hb : hauteur du point de référence en arrière-plan ; Ei : érosion initiale. 2 : **période d'érosion avancée.** Ht : hauteur du sommet de la butte couverte de lave ; Hp : hauteur du contact pré-volcanique/volcanique. Emax est l'érosion calculée à partir de la position estimée du contact volcanique/pré-volcanique (paléo-surface) ; Emax2 est l'érosion calculée en estimant que le sommet de la séquence désigne la paléo-surface (un lac de lave remplissant le cratère). Les nombres 1, 2, 3, 4 représentent les unités de roches pré-volcaniques. LD : coulées de lave et/ou dykes ; MCR : bancs pyroclastiques du rebord de cratère de maar ou d'anneau de tuff ; S : lits de scories ; VF : formations pyroclastiques remplissant un cratère ; EL : ligne d'érosion ; TC : contour incliné de la cheminée volcanique.

relatively high accidental lithic fragment contents, abundance of originally deep-seated accidental lithic clasts, presence of collapsed and subsequently inward subsided,

red at valley level and ca. 1 km at ridge level (Craw, 1985). The erosion rates calculated from diatremes of WVF similarly to other geological erosion estimates (Craw, 1985),

steeply dipping units and, in moderate stages of erosion, the presence of lacustrine and/or fluvial volcaniclastic units may support a maar origin of the erosional remnant.

The calculation of the erosion can be summarised in three major steps: 1) the original landform has to be reconstructed based on available field data; 2) the possible stage of erosion should be estimated from the mapped lithofacies associations, their facies relationships, thickness, relative abundance and position, and; 3) the possible "missing" pre-volcanic units and their thickness should be established based on the accidental lithic-clast population of exposed and mapped pyroclastic units of the erosional remnants.

The erosion rate calculations from the Miocene Waipiata Volcanic Field (New Zealand) indicate a range of a few tens of meters per million years erosion rate. Erosion rates based on volcanic remnants located close to a subsequently uplifted fault/fold block ("The Crater" and Black Rock) gave higher values of erosion (30 - 46 m/My) than calculations based on volcanic remnants located far from an uplifted fault/fold block (Swinburn - 3.75 - 15.6 m/My). Erosion rate calculations in Otago, based on a combination of study of 1) schistosity of the Otago Schist, 2) metavolcanic marker horizons, 3) position of boundary between schist zones, 4) position of Miocene erosion surfaces, and 5) estimated depth of exposure of lamprophyre diatremes gave similar erosion rates to those ones presented in this paper (Craw, 1995). An erosion estimate ~100 km west of the WVF on top of the uplifted Pisa Range gave less than 500 m of late Cenozoic erosion which number is in the same range (Craw, 1985) than the previously calculated rates from the uplifted Taieri Ridge (The Crater diatreme - 400 m) or other uplifted fault/fold blocks in eastern Otago (Black Rock diatreme - 550 m). Erosion inferred to be increased westward toward the Southern Alps, where ca. 3 km of erosion has occur-

gave significantly lower erosion values than fission track methods (Kamp and Tippett, 1993; Tippett and Kamp, 1993a,b). Fission track methods gave erosion >4 km but <8 km (Kamp and Tippett, 1993; Tippett and Kamp, 1993a,b) which value seems to be an overestimate, and cannot be supported by geological evidences (Craw, 1995). As it suggested earlier (Craw, 1995) and presented and supported in this study the erosion discrepancy between fission track and other geological estimates needs further explanation.

The erosion can be calculated in two different ways and both are recommended in cases of subsequent tilting since volcanism ceased. Firstly, if there is no evidence to support post-volcanic tilting, the first non-tilting model applies. Calculation of elevation differences between background and erosional remnant reference points should be corrected by estimated X values, according to the stage of erosion (tab. 1) or an estimation should be done based on the thickness of eroded pre-volcanic units according to the accidental

lithic-clast populations of the preserved pyroclastic rocks. Secondly, if volcanism was followed by any type of tilting, tilting should be considered and the erosion should be calculated using tilted models. Tilting can occur either immediately after or long after volcanism. If tilting occurred immediately after volcanism, erosion destroys a predominantly tilted landscape. If volcanism is followed by significant erosion and tilting occurs relatively long after volcanism, the present morphology is likely to be a result of the tilting rather than the erosion, therefore the effect of tilting should be accounted for in erosion rate calculations (2nd or 3rd model). Using a "tilted model", calculated erosion (E) will be significantly lower than erosion calculated using a non-tilted model (E_{max} or E_{max2}).

Acknowledgement

Thanks are due to J.D.L. White and A. Reay (University of Otago, Dunedin, New Zealand) for their suggestions on

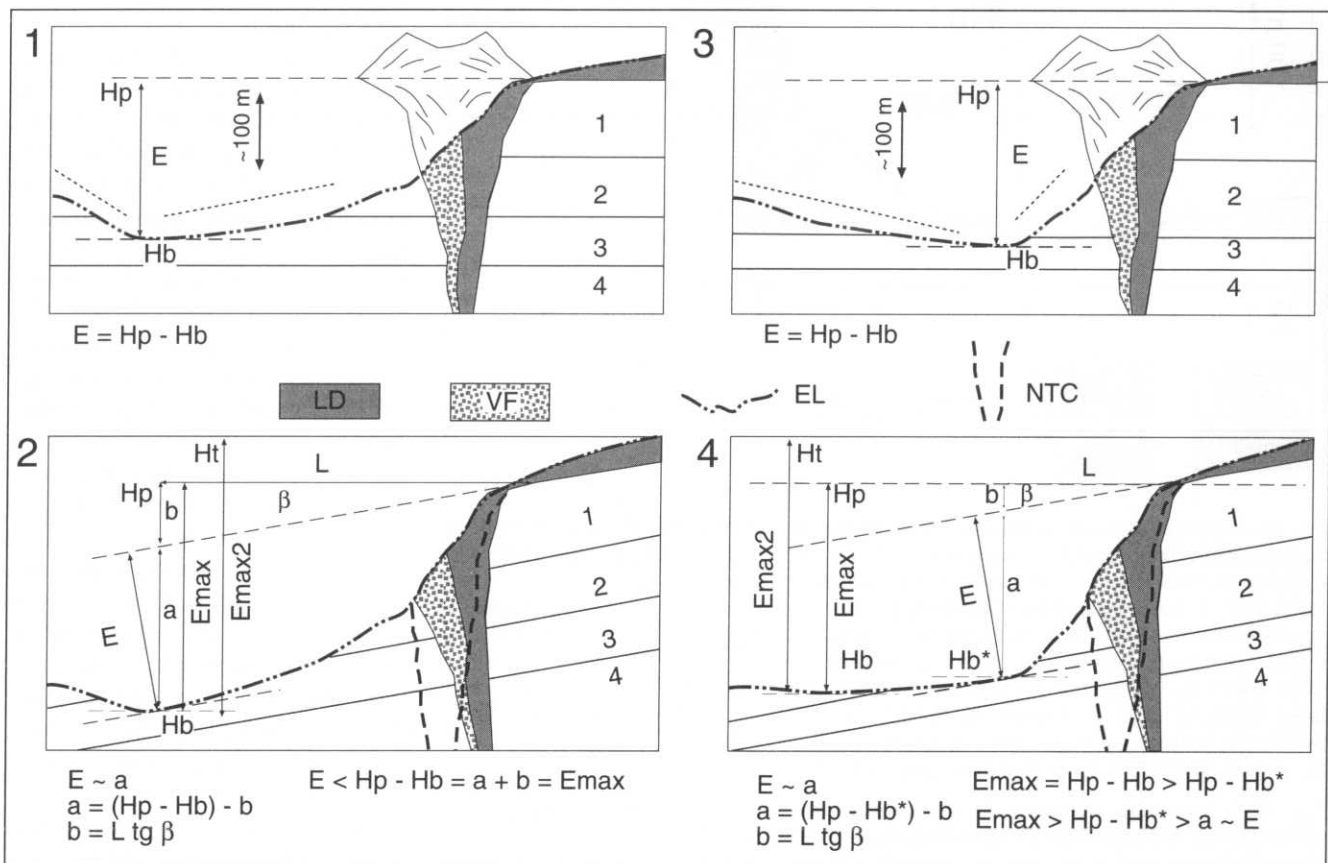


Fig. 11 – **Steps of erosion calculation methods on lava-capped scoria cone with phreatomagmatic base. Tilted model.** Tilting occurred after a major erosion phase lowered the region significantly. 1 and 2 show the stages of erosion in a case when erosion created a landscape with a lower slope angle towards the volcano; 3 and 4 show the steps of erosion when the created landscape has higher slope angle towards the volcano. 1 and 3 show the initial stage respectively. L is a distance between the background and erosional remnant reference points, b is a tilting angle. Numbers represent pre-volcanic rock units. LD: lava flows and/or dykes; VF: vent filling pyroclastic units; EL: erosion line; NTC: non-tilted contour of volcanic conduit.

Fig. 11 – Étapes des méthodes de calcul sur un cône de scories recouvert de lave avec une base phréatomagmatique. Modèle basculé. La déformation a eu lieu après qu'une phase majeure d'érosion eut abaissé la région de façon significative. 1 et 2 montrent les étapes de l'érosion dans le cas où celle-ci a créé un modèle avec une pente moins forte vers le volcan ; 3 et 4 montrent les étapes de l'érosion lorsque le modèle créé a une pente plus importante vers le volcan. 1 et 3 montrent respectivement la période initiale. L est la distance entre l'arrière-plan et les points de référence de l'édifice érodé, b est l'angle du basculement. Les nombres représentent les unités de roches pré-volcaniques. LD : coulées de lave et/ou dykes ; VF : formations pyroclastiques remplissant l'événement ; EL : ligne d'érosion ; NTC : enveloppe de la cheminée volcanique non basculée.

volcanism in Otago. The help of U. Martin (TU Bergakademie, Freiberg, Germany) both in field work and finalising the manuscript is greatly appreciated. The manuscript greatly benefited from suggestions by Journal reviewers, C. Pain (Australian Geological Survey Organization, Canberra, Australia), B.W. Hayward (University of Auckland, New Zealand) and J.-C. Thouret (University of Clermont-Ferrand, France). Thanks to M. McClintock (University of Otago, Dunedin) for improving the manuscript and to J-B. Rosseel for the French translations.

References

- Beget J.E., Hopkins D.M., Charron S.D. (1996)** – The largest maars on Earth, Seward Peninsula, northwest Alaska. *Arctic*, 49, 62-69.
- Büchel G. (1993)** – Maars of the Westeifel, Germany. In Negendank, J.F.W., Zolitschka, B. (Eds.): *Paleolimnology of European Maar Lakes*, 49, 1-13.
- Carter R.M. (1988)** – Plate boundary tectonics, global sea-level changes and the development of the eastern South Island continental margin, New Zealand, Southwest Pacific. *Marine and Petroleum Geology*, 5, 90-108.
- Coombs D.S., Reay A. (1986)** – Cenozoic alkaline and tholeiitic volcanism, eastern South Island, New Zealand. Days 1 to 4. Dunedin Volcanic Group, Waiareka-Deborah Volcanics, Timaru Basalt. Excursion C2. In (Ed.): *Fieldtrip guide-International Volcanological Congress*, 73.
- Cooper A.F., Barreiri B.A., Kimbrough D.L., Mattinson J.M. (1987)** – Lamprophyre dyke intrusion and the age of the Alpine Fault, New Zealand. *Geology*, 15, 941-944.
- Craw D. (1985)** – Structure of the schist in the Mt Aspiring region, northwestern Otago. *New Zealand Journal of Geology and Geophysics*, 28, 55-75.
- Craw D. (1995)** – Reinterpretation of the erosion profile across the southern portion of the Southern Alps, Mt Aspiring area, Otago, New Zealand. *New Zealand Journal of Geology and Geophysics*, 38, 501-507.
- Dohrenwend J.C., Wells B.D., Turrin B.D. (1986)** – Degradation of Quaternary cinder cones in the Cima volcanic field, Mojave Desert, California. *Geological Society of America Bulletin*, 97, 421-427.
- Fisher R.V., Schmincke H.-U. (1984)** – *Pyroclastic Rocks*. Springer. Heidelberg, 474 p.
- Gevrek A.I., Kazancı N. (2000)** – A Pleistocene, pyroclastic-poor maar from central Anatolia, Turkey: influence of a local fault on a phreatomagmatic eruption. *Journal of Volcanology and Geothermal Research*, 95, 309-317.
- Heiken G.H. (1971)** – Tuff rings: examples from the Fort Rock-Christmas Lake Valley Basin, South-Central Oregon. *Journal of Geophysical Research*, 76, 5615-5626.
- Kamp P.I.J., Tippett J.M. (1993)** – Dynamics of Pacific plate crust in the South Island (New Zealand) zone of oblique continent-continent convergence. *Journal of Geophysical Research*, 98, 16, 105-16, 118.
- LeMasurier W.E., Landis C.A. (1996)** – Mantle-plume activity recorded by low-relief erosion surface in West Antarctica and New Zealand. *Geological Society of America Bulletin*, 108, 1450-1466.
- Lorenz V. (1986)** – On the growth of maars and diatremes and its relevance to the formation of tuff rings. *Bulletin of Volcanology*, 48, 265-274.
- Lorenz V. (2000a)** – Formation of maar-diatreme volcanoes. *Terra Nostra*, 2000/6, 284-291.
- Lorenz V. (2000b)** – Formation of the root zones of maar-diatreme volcanoes. *Terra Nostra*, 2000/6, 279-284.
- Lorenz V., Mc Birney A.R., Williams H. (1970)** – *An investigation of volcanic depressions. Part III. Maars, tuff-rings, tuff-cones and diatremes*. Clearinghouse for Federal Scientific and Technical Information, Springfield, Va. Houston, Texas, 196 p.
- McDougall I., Coombs D.S. (1973)** – Potassium-Argon ages for the Dunedin Volcano and outlying volcanics. *N.Z. Journal of Geology and Geophysics*, 16, 179-188.
- Mertes H. (1983)** – Aufbau und Genese des Westeifeler Vulkanfeldes. *Bochumer Geol. und Geotechn. Arb.*, 9, 1-415.
- Németh K. (2000)** – Collapse structures of an eroded maar/diatreme volcanic field from Central Otago, New Zealand: The Crater as an example. *Terra Nostra*, 6, 364-375.
- Németh K. (2001)** – Phreatomagmatic volcanism of the Waipiata Volcanic Field, New Zealand in comparison with Bakony- Balaton Highland Volcanic Field, Hungary. *Geology Department. University of Otago. Dunedin, New Zealand*. PhD thesis.
- Németh K., Martin U. (1999)** – Late Miocene paleo-geomorphology of the Bakony-Balaton Highland Volcanic Field (Hungary) using physical volcanology data. *Zeitschrift für Geomorphologie N.F.*, 43, 417-438.
- Németh K., Martin U., Harangi S. (2000)** – On the calculation of the geometry of the diatreme pipe from a deposits of an "accidental lithic clast rich" maar, Tihany East Maar (Hungary). *Terra Nostra*, 6, 383-391.
- Schmincke H.-U. (1977)** – Phreatomagmatische Phasen in quaternären Vulkanen der Osteifel. *Geologische Jahrbuch*, A 39, 3-45.
- Sohn Y.K. (1996)** – Hydrovolcanic processes forming basaltic tuff rings and cones on Cheju Island, Korea. *Geological Society of America Bulletin*, 108, 1199-1211.
- Thouret J.-C. (1999)** – Volcanic geomorphology-an overview. *Earth Sciences Review*, 47, 95-131.
- Tippett J.M., Kamp P.I.J. (1993a)** – Fission track analysis of the late Cenozoic vertical kinematics of continental Pacific crust, South Island, New Zealand. *Journal of Geophysical Research*, 98, 16, 119-16,148.
- Tippett J.M., Kamp P.I.J. (1993b)** – The role of faulting in rock uplift in the Southern Alps, New Zealand. *New Zealand Journal of Geology and Geophysics*, 36, 497-504.
- Vespermann D., Schmincke H.-U. (2000)** – Scoria cones and tuff rings. In Sigurdsson H., Houghton B.F., McNutt S.R., Rymer H., Stix J. (Eds.): *Encyclopedia of Volcanoes*, 683-694.
- White J.D.L. (1990)** – Depositional architecture of a maar-pitted playa: sedimentation in the Hopi Buttes volcanic field, northeastern Arizona, U.S.A. *Sedimentary Geology*, 67, 55-84.
- White J.D.L. (1991)** – The depositional record of small, monogenetic volcanoes within terrestrial basins. In: Fisher R.V. & Smith G.A. (Eds.): *Sedimentation in Volcanic Settings*, 45, 155-171.
- White J.D.L. (1992)** – Pliocene subaqueous fans and Gilbert-type deltas in maar crater lakes, Hopi Buttes, Navajo Nation (Arizona), USA. *Sedimentology*, 39, 931-946.